Structure and energetics of $LaAlO_3$ (001) surfaces

K. Krishnaswamy
Department of Electrical and Computer Engineering, University of California, Santa Barbara, California 93106-9560, USA

C. E. Dreyer, A. Janotti, and C. G. Van de Walle
Materials Department, University of California, Santa Barbara, California 93106-5050, USA

(Received 27 January 2014; revised manuscript received 5 October 2014; published 29 December 2014)

Reconstructions of the $LaAlO_3$ (001) surface are studied using hybrid density functional calculations. We calculate surface energies as a function of O and Al chemical potentials for both the LaO- and AlO_2-terminated surfaces. We find that the (3×2) Al adatom is the most stable reconstruction on the AlO_2 termination, with the (2×2) O vacancy slightly higher in energy. On the LaO termination, the (3×2) La vacancy is the most stable reconstruction. Overall, the LaO termination with the (3×2) La vacancy has the lowest surface energy, in the absence of impurities. However, our calculations also indicate that the presence of hydrogen alters the stability of the LaO *versus* the AlO_2 termination. Under Al-rich conditions, H binds to an O atom forming a (2×1) H-adatom reconstruction on the AlO_2-terminated surface, whereas under La-rich conditions a (2×1) OH adsorbate reconstruction forms on the LaO-terminated surface. These reconstructions are found to be the most stable terminations over a wide range of H and O chemical potentials.

DOI: 10.1103/PhysRevB.90.235436 PACS number(s): 68.35.B−, 73.20.−r, 71.15.Mb

I. INTRODUCTION

$LaAlO_3$ (LAO) is an insulator with a band gap of ∼5.6 eV [1] that crystallizes in the perovskite structure. It is widely used as a substrate for high-T_c superconductor [2] and colossal magnetoresistive materials [3], and is also considered as a high-k dielectric for metal-oxide-semiconductor field effect transistors (MOSFETs) [4,5]. The demonstration of a high-density two-dimensional electron gas (2DEG) at the interface between LAO and a $SrTiO_3$ (STO) (001) substrate [6,7] has also raised interest. Whether as a substrate or as a thin film, the surface termination of LAO is expected to affect the behavior and performance of LAO in these applications. For instance, it has been proposed that the surface of the LAO layer strongly affects the properties of the 2DEG at the LAO/STO interface [8–11]. In spite of its relevance, the stable termination, reconstructions, and surface energetics of the LAO surface are still poorly understood [5,12–22].

Along the [001] direction, LAO can be viewed as composed of alternating planes of LaO and AlO_2, as shown in Fig. 1. Some experiments on bulk crystals have indicated that the (001) surface is terminated on either LaO or AlO_2 planes, depending on the annealing temperature [12,13,16], while others have suggested that both terminations are present simultaneously [14,18]. It has also been proposed, based on a combination of first-principles calculations and transmission electron diffraction, that the LAO surface exhibits a $(\sqrt{5}\times\sqrt{5})R26^\circ$ reconstruction with an excess of delocalized holes [17]. This result is puzzling because the valence band in LAO is very low in energy with respect to the vacuum level [23,24]; holes on the surface are therefore energetically unfavorable.

Here, we use first-principles calculations based on density functional theory (DFT) and a hybrid functional to investigate the possible reconstructions and determine the surface energies for both LaO and AlO_2 terminations of the $LaAlO_3$ (001). LAO has a rhombohedral perovskite structure at room temperature [1] and transforms into a cubic phase at ∼813 K [25]. The rhombohedral phase of LAO has a pseudo-cubic lattice constant $a = 3.790$ Å and exhibits only a small deviation (by angles of a few tenths of a degree) from the cubic structure [25]. Furthermore, the calculated values of the enthalpy of formation for the cubic and rhombohedral phases differ by only 24 meV/(formula unit). We therefore expect the surface reconstructions of the rhombohedral phase to be very similar to those of the cubic structure, and in the present study, we have focused on the cubic phase.

II. COMPUTATIONAL APPROACH

Our calculations are based on density functional theory [26,27] with the screened hybrid functional of Heyd, Scuseria, and Ernzerhof (HSE) [28,29], and the projector augmented wave method [30,31] as implemented in the VIENNA *ab initio* simulation package (VASP) [32–34]. A systematic comparison between the generalized gradient approximation (GGA) [35] and HSE showed that surface energy values calculated using GGA were not sufficiently accurate, and at times led to qualitative changes in the relative stability of different reconstructions. The LAO surfaces were studied using a slab geometry with periodic boundary conditions. Each slab has a thickness of 5.5 unit cells and two identical surfaces. A 1.5-unit-cell thick region at the center of the slab was kept fixed to the LAO bulk structure, while atoms within two unit cells of each surface were allowed to relax. The slabs were separated by a vacuum region of thickness ∼15 Å for vacancy reconstructions and ∼23 Å for adatom reconstructions (measured between surface planes). Integrations over the Brillouin zone were performed using a 4×4×1 mesh for the unreconstructed surface, 2×4×1 for the 2×1 reconstruction (see Fig. 1), and 2×2×1 for the 2×2 and 3×2 reconstructions. The plane-wave basis set had a cutoff of 500 eV. Convergence with respect to k-point sampling, as well as slab and vacuum thickness was explicitly checked. In order to minimize systematic errors due to k-point sampling in the calculations of surface energies, we

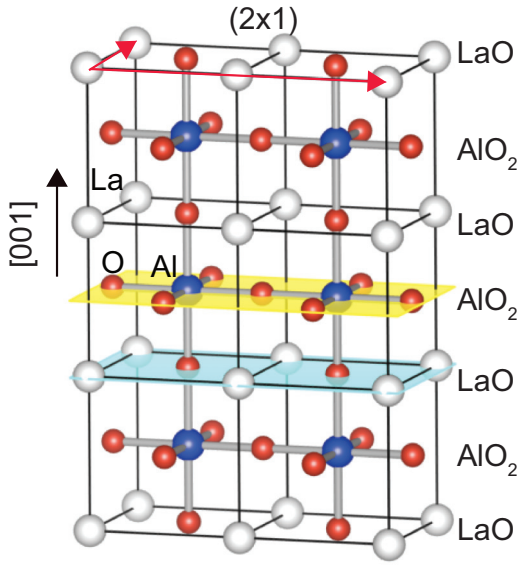

FIG. 1. (Color online) Cubic perovskite crystal structure of $LaAlO_3$ (LAO) viewed as alternating planes of LaO and AlO_2 along the [001] direction. The lattice vectors for a 2×1 unit cell of the LAO (001) surface are indicated on the top surface.

calculated formation energies based on bulk supercells with the same in-plane periodicity and k-point mesh as for the slab supercells.

The surface energy for a given reconstruction is determined by

$$\sigma_{\text{surface}} = \tfrac{1}{2}[E_{\text{slab}}(n_{\text{LAO}}) - E_{\text{bulk}}(n_{\text{LAO}}) - n_{\text{La}}\mu_{\text{La}} - n_{\text{Al}}\mu_{\text{Al}} - n_{\text{O}}\mu_{\text{O}}], \quad (1)$$

where E_{slab} is the total energy of the slab supercell containing two identical surfaces, $E_{\text{bulk}}(n_{\text{LAO}})$ is the total energy of the corresponding number of bulk LAO cells, n_i is the number of excess atoms of species i in the slab supercell, and μ_i is the chemical potential of species i.

The chemical potentials μ_i are variables, and can be set to represent experimental conditions. The allowed range of variation of μ_i is determined by the stability of LAO. If we reference the chemical potentials to the corresponding elemental phases (i.e., the elemental metal for Al and La, and an isolated O_2 molecule for O), the stability of LAO is given by

$$\mu_{\text{Al}} + \mu_{\text{La}} + 3\mu_{\text{O}} = \Delta H_f(\text{LaAlO}_3), \quad (2)$$

where $\Delta H_f(\text{LaAlO}_3)$ is the enthalpy of formation of LAO. Thus the three chemical potentials cannot be varied independently; fixing the values for two of the constituents will specify the third. Further restrictions are imposed due to formation of competing phases such as Al_2O_3 and La_2O_3. In the Al-rich limit, we have

$$2\mu_{\text{Al}} + 3\mu_{\text{O}} \leqslant \Delta H_f(\text{Al}_2\text{O}_3), \quad (3)$$

while in the La-rich regime, the limit is set by the formation of La_2O_3:

$$2\mu_{\text{La}} + 3\mu_{\text{O}} \leqslant \Delta H_f(\text{La}_2\text{O}_3). \quad (4)$$

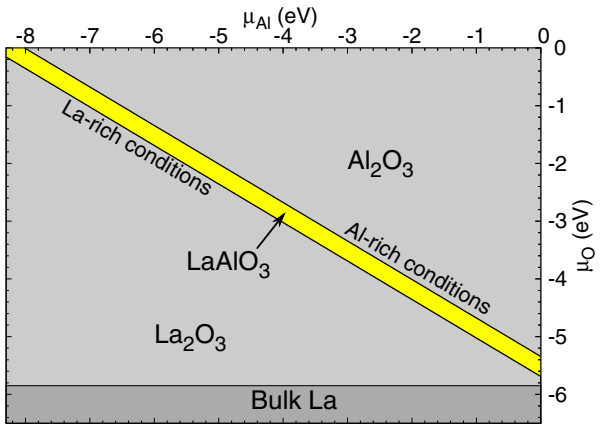

FIG. 2. (Color online) Phase diagram depicting stability of $LaAlO_3$ as a function of μ_{Al} and μ_{O}. The phase boundaries are indicated as Al-rich and La-rich conditions during growth of $LaAlO_3$.

The limits imposed by the formation of Al_2O_3 and La_2O_3 can be represented in a phase diagram (Fig. 2). At each (μ_{Al}, μ_{O}) point in this diagram, μ_{La} is given by Eq. (2). Our calculated enthalpies of formation are listed in Table I along with the experimental values for comparison.

For any μ_{O} value, the Al-rich condition under which LAO is stable is given by the value of μ_{Al} on the line separating the LAO region from the Al_2O_3 region, as indicated in Fig. 2, while the La-rich limit is given by the μ_{Al} values on the line separating the LAO region from the La_2O_3 region. Therefore the choice of Al-rich or La-rich limit specifies the μ_{Al} and the μ_{La} for a given μ_{O}, where all three variables are connected by Eq. (2). In the discussion below, we present results for surface energies with respect to μ_{O} for both Al-rich and La-rich limiting conditions.

III. SURFACE RECONSTRUCTIONS

The La and Al atoms each contribute three valence electrons, assuming a +3 charge, while O assumes a –2 charge. Thus, in the bulk, a LaO plane ($La^{+3}O^{-2}$) has a net charge of –1 per unit cell, whereas a AlO_2 plane ($Al^{+3}O_2^{-2}$) has a charge of +1 per unit cell. Along the [001] direction, we can think of each LaO-plane donating $1/2\ e^-$ per unit cell to the AlO_2 plane above and $1/2\ e^-$ to the AlO_2 plane below. Therefore the electron counting shows that the unreconstructed (1×1) LaO-terminated surface results in an excess of $1/2\ e^-$ per unit cell area due to the lack of an AlO_2 plane above to accept the excess electrons. An inspection of the surface electronic structure shows that the excess electrons are accommodated

TABLE I. Enthalpy of formation (ΔH_f), in units of eV/(formula unit), for La_2O_3, Al_2O_3, and $LaAlO_3$.

	Enthalpy of formation, ΔH_f	
Material	Calculated	Experimental
La_2O_3	−18.0	−18.57 [Ref. 36]
Al_2O_3	−16.0	−17.37 [Ref. 37]
$LaAlO_3$	−17.6	−18.69 [Ref. 38]

in surface states near the conduction band, derived from La $5d$ states. On the other hand, the unreconstructed (1×1) AlO_2-terminated surface results in a deficit of $1/2$ electron (or, equivalently, an excess of $1/2$ hole) per unit cell area. These excess holes occupy surface states near the valence band. Both types of unreconstructed surface are therefore energetically unfavorable, given that the O $2p$-derived valence band of LAO is low in energy relative to the vacuum level (raising the cost of holes in states near the valence band), and the La $5d$-derived conduction band is high in energy (making electrons in states near the conduction band energetically costly). Therefore it is reasonable to expect the stable reconstructions to obey electron counting [39] and result in an insulating surface.

For the LaO termination, we thus expect the stable surface reconstructions to involve acceptorlike surface states near the valence band that accommodate the excess electrons. In the case of the AlO_2 termination, we expect the stable surface reconstructions to exhibit donorlike states to fill up the holes in the surface states near the valence band. This explains why previous studies [20–22] of LAO on STO find low formation energies for donor-type point defects such as the O-vacancy at the AlO_2 surface. Calculations in these studies of point-defect formation have been carried using supercells with surface areas [20,21] $(1\times1, 2\times2,$ or $3\times2)$ that are too small to address single, isolated point defects on the surface. Such structures should be effectively regarded as surface reconstructions, which is the subject of the present paper.

The calculated surface energies are summarized in Table II. These reconstructions result in surfaces with the stoichiometry of the limiting phases, so their surface energies are independent of μ_O. The surface energies of the lowest energy reconstructions, under Al-rich and La-rich conditions, are plotted in Fig. 3. The unreconstructed AlO_2 and LaO terminations are also shown for comparison. These agree well with the results of Sorokine *et al.* [19], which addressed only unreconstructed surfaces. We find the most stable reconstruction for the LaO termination to consist of a La vacancy per (3×2) surface cell. The removal of a La atom results in three holes in states near the valence band. Since the unreconstructed (1×1) LaO-terminated surface has an excess of $1/2$ electron per unit cell area, one La vacancy per 3×2 cell leads to complete transfer of the electrons in states near the conduction band to states near the valence band. The net result is an insulating surface that satisfies the electron counting rule [39], with an atomic structure as shown in Fig. 4(d). We have also considered a (2×2) O-adatom reconstruction. The O adatom accepts two electrons, again resulting in an insulating surface. The adatom sits on top of a La atom on the LaO-terminated surface. However, the (2×2) O-adatom reconstruction is higher in energy than the (3×2) La-vacancy reconstruction by 46 meV/Å^2 under Al-rich and 41 meV/Å^2 under La-rich conditions.

For the AlO_2 termination, we find that the most stable reconstruction consists of one Al adatom per 3×2 surface cell, with the extra Al atom occupying one of the La sites in the layer above the surface as shown in Fig. 4(a). The (3×2) Al-adatom results in an insulating surface based on electron counting. We find that a (3×2) La-adatom reconstruction also leads to an insulating surface, but it is higher in energy than the (3×2) Al-adatom reconstruction by 15 meV/Å^2 in the Al-rich and by 3 meV/Å^2 in the La-rich limits. An O vacancy per 2×2 cell

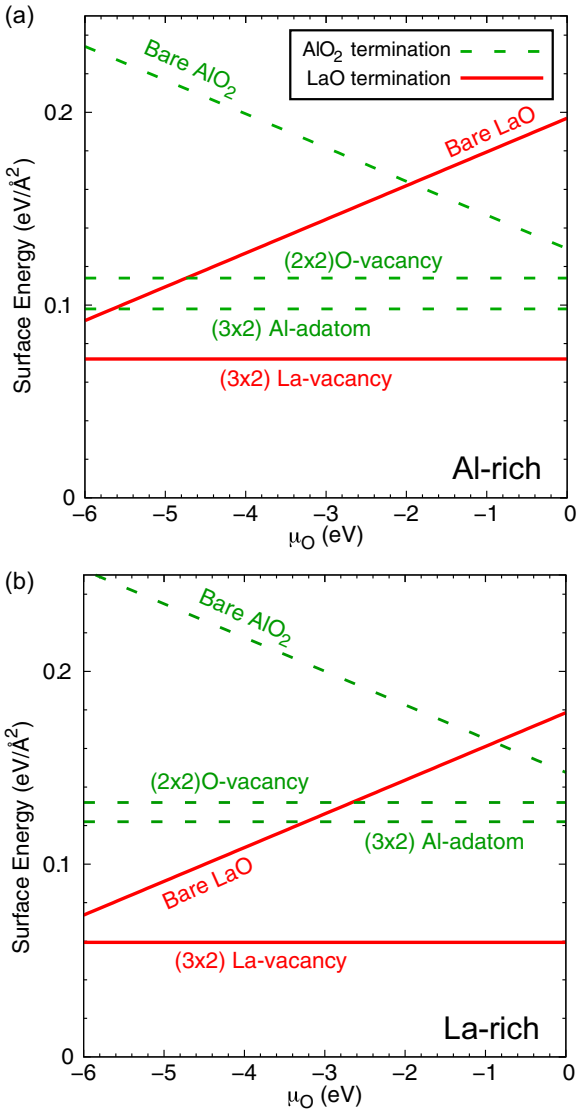

FIG. 3. (Color online) Surface energy per unit area for various reconstructions on the $LaAlO_3$ surface as a function of μ_O, under (a) Al-rich and (b) La-rich conditions. Solid (red) lines refer to LaO termination, whereas the dashed (green) lines refer to AlO_2 termination.

TABLE II. Surface energies (in meV/Å^2) for selected reconstructions on the $LaAlO_3$ (001) surface, under Al- and La-rich conditions.

		$\sigma_{surface}$ (meV/Å^2)	
Termination	Reconstruction	Al-rich	La-Rich
AlO_2	(2×2) O vacancy	114	132
	(3×2) Al adatom	98	122
	(3×2) La adatom	113	125
	(2×1) Al+O adatom	255	292
LaO	(3×2) La vacancy	72	59
	(2×2) O adatom	118	100

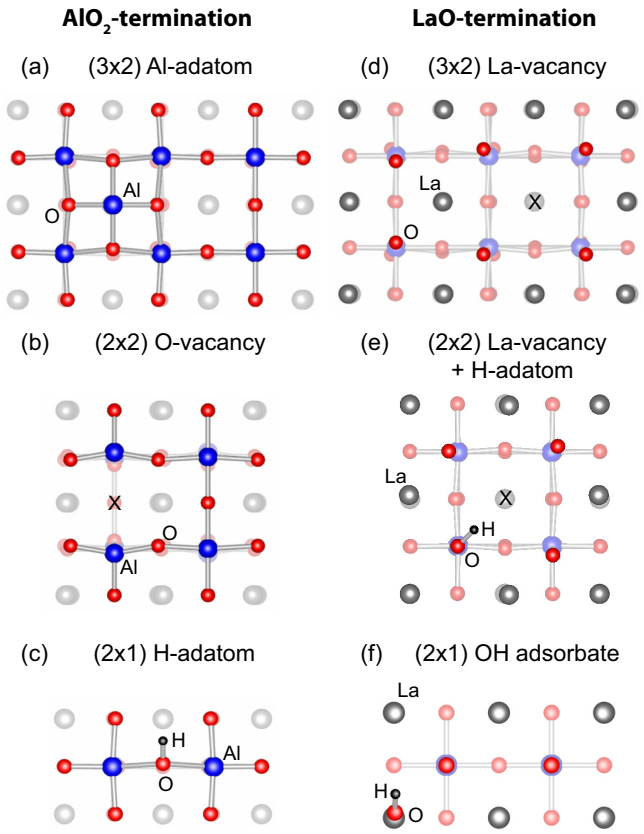

FIG. 4. (Color online) Top view of the lowest-energy reconstructions on the $LaAlO_3$ (001) surface. For the AlO_2 termination we show the (a) (3×2) Al-adatom, (b) (2×2) O-vacancy, and (c) (2×1) H-adatom reconstructions. For the LaO termination, we show the (d) (3×2) La-vacancy, (e) (2×2) La vacancy with H adatom, and (f) (2×1) OH adsorbate reconstructions.

on the AlO_2 termination [Fig. 4(b)] also satisfies the electron counting rule, since an O vacancy results in two electrons associated with two Al dangling bonds, which lie high in the band gap. Still, the (2×2) O-vacancy reconstruction is also higher in energy than the (3×2) Al-adatom reconstruction, by 16 meV/Å^2 under Al-rich and 10 meV/Å^2 under La-rich conditions.

Overall, we find the (3×2) La-vacancy reconstruction on the LaO termination to be the most stable surface for $LaAlO_3$. *A posteriori*, this can be explained by considering the nature of the chemical bonds in LAO. One can think of LAO as composed of AlO_3^{-3} units forming a backbone of AlO_6 octahedra, with La^{+3} ions occupying a cubic lattice. Therefore removing a La atom does not lead to bond rupture and costs less energy. On the other hand, removing an Al or O atom results in dangling bonds, since the Al-O bonds have strong covalent character and breaking them usually requires more energy than breaking ioniclike bonds.

IV. EFFECT OF ADATOMS AND ADSORBATES

The results above indicate that the LAO surface of bulk crystals should be LaO terminated with a (3×2) La-vacancy

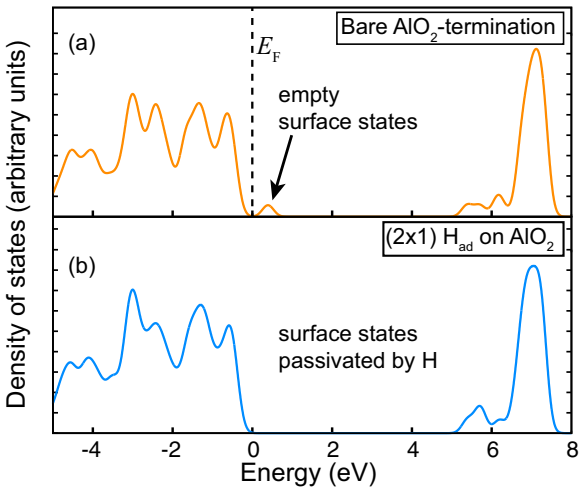

FIG. 5. (Color online) Density of states plot showing (a) the presence of empty states near the valence band for the bare AlO_2 termination, and (b) the passivation of these surface states by H acting as a donor in a (2×1) H-adatom reconstruction on the AlO_2 termination.

reconstruction, in both La-rich and Al-rich limits. This seems contradictory to experimental observations that the surface termination can be tuned based on the conditions to which the surface is exposed [18]. One possible reason for the change in termination may be the influence of impurities such as hydrogen on the surface, which was observed by Yao *et al.* in their time-of-flight scattering experiment [14]. We note that hydrogen is present in almost all growth and annealing environments, and H is expected to form a strong bond with any O atoms that are exposed at the surface. The O-H bond results in an excess electron if the O atom already has a closed $2p$ shell through bonding with other host atoms. Because of this donorlike character, the surface energy of the AlO_2 termination, which has empty surface states near the valence band, is expected to decrease upon hydrogenation. In the same way, reconstructions on the LaO termination with more than one La vacancy per (3×2) cell will result in holes that could be filled upon hydrogenation.

To test these possibilities, we calculated the (2×1) H-adatom reconstruction on the AlO_2 termination [shown in Fig. 4(c)] and the (2×2) La-vacancy with an H-adatom reconstruction on the LaO termination [shown in Fig. 4(e)]. The density of states calculated for the bare AlO_2-termination surface [shown in Fig. 5(a)] exhibits empty surface states near the valence band. When the H adatom forms a (2×1) reconstruction, these surface states become completely filled [shown in Fig. 5(b)], establishing the donorlike character of the H adatom.

We also considered a reconstruction with OH adsorbates, which can accept one electron. On the LaO termination, OH adsorbates give rise to a (2×1) reconstruction [shown in Fig. 4(f)] that satisfies the electron counting rule. We find that the OH molecule takes away the excess electron from the (2×1) LaO termination, becoming OH^-, and sits on top of a surface La atom with a distance of about 2.18 Å between the La and the O, and an O-H bond distance of 0.96 Å. No distortion of the charge density surrounding the OH- ion due

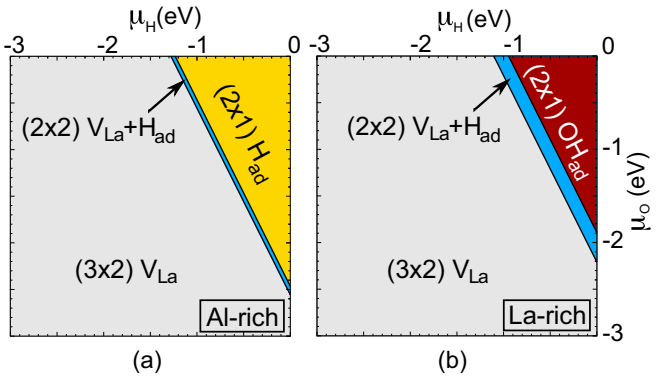

FIG. 6. (Color online) Stability of the (3×2) La vacancy (V_{La}) [shown in light gray], the (2×2) La vacancy with H adatom (V_{La}+H_{ad}) [shown in blue], and the (2×1) OH adsorbate (OH_{ad}) [shown as dark red] reconstructions on the LaO termination vs the (2×1) H-adatom (H_{ad}) reconstruction on the AlO_2 termination [shown in yellow] as a function of μ_H and μ_O, under (a) Al-rich and (b) La-rich conditions.

to the La atom was evident, suggesting that the interaction is ionic in nature. We note that H_2O, owing to its large gap between occupied and unoccupied states, will not result in any electron transfer to passivate the excess holes/electrons occurring on the bare LAO surfaces, and hence does not lead to stable reconstructions.

From a comparison between the three H-based reconstructions studied here and the most stable native (3×2) La-vacancy reconstruction shown in Fig. 6, we find the (2×1) H-adatom reconstruction on the AlO_2 termination to have the lowest surface energy under Al-rich and moderately O-rich conditions. Under La-rich conditions, on the other hand, the (2×1) OH adsorbate reconstruction on the LaO termination has the lowest surface energy. Therefore, in the presence of H, Al-rich conditions favor the AlO_2 termination, while La-rich conditions favor the LaO termination.

V. DISCUSSION

Kawanowa *et al.* [18] observed that LAO substrate in ultrahigh vacuum (10^{-7} mbar) at 1000 K (corresponding to $\mu_O = -2.0$ eV, if we assume $p_{O_2} = 10^{-7}$ mbar) results in LaO termination, while room-temperature samples show AlO_2 termination. Annealing the samples at high temperatures brings the surface closer to thermodynamic equilibrium, and the observed termination at high temperature is indeed consistent with our results, which show the LaO termination with a (3×2) La-vacancy reconstruction to be most stable. We suggest that the observed AlO_2 termination at room temperature results from stabilization by hydrogen adatoms. The adsorption of other donorlike impurities on the surface would similarly favor the AlO_2-terminated surface over the LaO termination.

Lanier *et al.* [17], using a combination of transmission electron diffraction measurements and density functional calculations, concluded that LAO single crystals terminate in the LaO surface with a $(\sqrt{5}\times\sqrt{5})R26^\circ$ reconstruction containing a La vacancy, i.e., one La vacancy per five unit cells. Note that this is close to the (3×2) La-vacancy reconstruction (i.e., one vacancy per six unit cells) and the (2×2) La-vacancy reconstruction with an H-adatom (i.e., one vacancy per four unit cells), both of which we find to be the most stable surface. The $(\sqrt{5}\times\sqrt{5})R26^\circ$ La-vacancy reconstruction leads to one missing electron (i.e., one hole) per ten unit cells, with the hole occupying an O $2p$-derived surface state near the valence band. In our view, such a reconstruction is unlikely to occur because of the high energy cost associated with holes in low-lying surface states. We suggest that the observed $(\sqrt{5}\times\sqrt{5})R26^\circ$ reconstruction contains a defect or impurity in addition to the La vacancy. Hydrogen is a likely candidate [17], since it would not alter the symmetry of the reconstruction and is generally difficult to detect experimentally.

Finally, in the case of thin LAO films deposited on STO (001) [6,7], the 2DEG at the STO/LAO interface affects the stability and reconstruction of the LAO top surface [8]. The electronic states occupied by the electrons in the 2DEG, which are STO conduction-band states, are much higher in energy than the O-derived valence bands [8]. For the thin LAO films used in the experiments, electrons from the 2DEG can be transferred to the surface, altering the relative stability of the reconstructions. In particular, electrons can fill the holes that would be present on an AlO_2-terminated unreconstructed surface, stabilizing this termination. Note that such a source of electrons is not available in the case of bulk substrates or thick LAO films, where transfer of electrons would be energetically too costly. Indeed, such a transfer of electrons from the interface to the surface carries an energy cost due to the resulting electric field across the LAO layer, and this cost must be included in an analysis of the overall stability of the heterostructure [11].

VI. CONCLUSION

In conclusion, we have studied different reconstructions of the LAO (001) surface and find that for bare surfaces of bulk samples (or thick films) a (3×2) La-vacancy reconstruction on the LaO-plane termination is most stable. The presence of impurities such as hydrogen can stabilize other reconstructions, such as the (2×1) H-adatom reconstruction for AlO_2 termination, and a (2×1) OH-adsorbate reconstruction or (2×2) La-vacancy reconstruction with an H adatom on the LaO termination. In the case of STO/LAO heterostructures, the unreconstructed AlO_2 termination is stabilized due to the availability of electrons from the interface to compensate the holes in low-lying surface states.

ACKNOWLEDGMENTS

This work was supported in part by the Center for Low Energy Systems Technology (LEAST), one of six SRC STARnet Centers sponsored by MARCO and DARPA, and by the U. S. Army Research Office under Grant No. W911-NF-11-1-0232. Computing resources were provided by the CSC/CNSI/MRL (an NSF MRSEC, DMR-1121053), supported by NSF CNS-0960316, and by XSEDE, supported by NSF OCI-1053575.

[1] S.-G. Lim, S. Kriventsov, T. N. Jackson, J. H. Haeni, D. G. Schlom, A. M. Balbashov, R. Uecker, P. Reiche, J. L. Freeouf, and G. Lucovsky, J. Appl. Phys. **91**, 4500 (2002).
[2] P. McIntyre and M. Cima, J. Mater. Res. **9**, 2219 (1994).
[3] Z. L. Wang and J. Zhang, Phys. Rev. B **54**, 1153 (1996).
[4] C. Tsai, T. Wu, and A. Chin, IEEE Electron Device Lett. **33**, 35 (2012).
[5] D. O. Klenov, D. G. Schlom, H. Li, and S. Stemmer, Jpn. J. Appl. Phys. **44**, L617 (2005).
[6] A. Ohtomo and H. Y. Hwang, Nature (London) **427**, 423 (2004).
[7] S. Thiel, G. Hammerl, A. Schmehl, C. W. Schneider, and J. Mannhart, Science **313**, 1942 (2006).
[8] A. Janotti, L. Bjaalie, L. Gordon, and C. G. Van de Walle, Phys. Rev. B **86**, 241108 (2012).
[9] Y. Xie, Y. Hikita, C. Bell, and H. Y. Hwang, Nat. Commun. **2**, 494 (2011).
[10] C. Cen, S. Thiel, G. Hammerl, C. W. Schneider, K. E. Andersen, C. S. Hellberg, J. Mannhart, and J. Levy, Nat. Mater. **7**, 298 (2008).
[11] N. C. Bristowe, P. B. Littlewood, and E. Artacho, Phys. Rev. B **83**, 205405 (2011).
[12] Z. L. Wang and A. J. Shapiro, Surf. Sci. **328**, 141 (1995).
[13] Z. L. Wang and A. J. Shapiro, Surf. Sci. **328**, 159 (1995).
[14] J. Yao, P. Merrill, and S. Perry, J. Chem. Phys. **108**, 1645 (1998).
[15] R. J. Francis, S. C. Moss, and A. J. Jacobson, Phys. Rev. B **64**, 235425 (2001).
[16] D.-W. Kim, D.-H. Kim, B.-S. Kang, T. W. Noh, D. R. Lee, and K.-B. Lee, Appl. Phys. Lett. **74**, 2176 (1999).
[17] C. H. Lanier, J. M. Rondinelli, B. Deng, R. Kilaas, K. R. Poeppelmeier, and L. D. Marks, Phys. Rev. Lett. **98**, 086102 (2007).
[18] H. Kawanowa, H. Ozawa, M. Ohtsuki, Y. Gotoh, and R. Souda, Surf. Sci. **506**, 87 (2002).
[19] A. Sorokine, D. Bocharov, S. Piskunov, and V. Kashcheyevs, Phys. Rev. B **86**, 155410 (2012).
[20] Y. Li, S. N. Phattalung, S. Limpijumnong, J. Kim, and J. Yu, Phys. Rev. B **84**, 245307 (2011).
[21] T. Jin-Long, J. Zhu, W.-F. Qin, J. Xiong, and Y.-R. Li, Chin. Phys. B **17**, 655 (2008).
[22] H. Seo and A. A. Demkov, Phys. Rev. B **84**, 045440 (2011).
[23] M. Choi, A. Janotti, and C. G. Van de Walle, Phys. Rev. B **88**, 214117 (2013).
[24] N. Goel, W. Tsai, C. M. Garner, Y. Sun, P. Pianetta, M. Warusawithana, D. G. Schlom, H. Wen, C. Gaspe, J. C. Keay, M. B. Santos, L. V. Goncharova, E. Garfunkel, and T. Gustafsson, Appl. Phys. Lett. **91**, 113515 (2007).
[25] S. A. Hayward, F. D. Morrison, S. A. T. Redfern, E. K. H. Salje, J. F. Scott, K. S. Knight, S. Tarantino, A. M. Glazer, V. Shuvaeva, P. Daniel, M. Zhang, and M. A. Carpenter, Phys. Rev. B **72**, 054110 (2005).
[26] P. Hohenberg and W. Kohn, Phys. Rev. **136**, B864 (1964).
[27] L. J. Sham and W. Kohn, Phys. Rev. **140**, A1133 (1965).
[28] J. Heyd, G. E. Scuseria, and M. Ernzerhof, J. Chem. Phys. **118**, 8207 (2003).
[29] J. Heyd, G. E. Scuseria, and M. Ernzerhof, J. Chem. Phys. **124**, 219906 (2006).
[30] P. E. Blöchl, Phys. Rev. B **50**, 17953 (1994).
[31] G. Kresse and D. Joubert, Phys. Rev. B **59**, 1758 (1999).
[32] G. Kresse and J. Hafner, Phys. Rev. B **47**, 558 (1993).
[33] G. Kresse and J. Furthmüller, Comput. Mater. Sci. **6**, 15 (1996).
[34] G. Kresse and J. Furthmüller, Phys. Rev. B **54**, 11169 (1996).
[35] J. P. Perdew, K. Burke, and M. Ernzerhof, Phys. Rev. Lett. **77**, 3865 (1996).
[36] E. Cordfunke and R. Konings, Thermochim. Acta **375**, 65 (2001).
[37] S. Zumdahl, *Chemical Principles* (Cengage Learning, Belmont, CA, USA, 2007).
[38] J. Cheng and A. Navrotsky, J. Mater. Res. **18**, 2501 (2003).
[39] G. P. Srivastava, Appl. Surf. Sci. **252**, 7600 (2006).